


Manipulating the non-Hermitian skin effect via electric fields

Yi Peng ^{*}, Jianwen Jie ^{*}, Dapeng Yu, and Yucheng Wang [†]

Shenzhen Institute for Quantum Science and Engineering, Southern University of Science and Technology,
Shenzhen 518055, China;

International Quantum Academy, Shenzhen 518048, China;

and Guangdong Provincial Key Laboratory of Quantum Science and Engineering, Southern University of Science and Technology,
Shenzhen 518055, China

 (Received 29 January 2022; revised 19 April 2022; accepted 28 September 2022; published 4 October 2022)

In non-Hermitian systems, the phenomenon that the bulk-band eigenstates are accumulated at the boundaries of the systems under open boundary conditions is called the non-Hermitian skin effect (NHSE), which is one of the most iconic and important features of a non-Hermitian system. In this work, we investigate the fate of the NHSE in the presence of electric fields by analytically calculating the dynamical evolution of an initial bulk state and numerically computing the spectral winding number and the distributions of eigenstates, as well as the dynamical evolutions. We show abundant manipulation effects of dc and ac fields on the NHSE and that the physical mechanism behind these effects is the interplay between the Stark localization, dynamic localization, and the NHSE. In addition, the finite size analysis of the non-Hermitian system with a pure dc field shows the phenomenon of size-dependent NHSE. We further propose a scheme to realize the discussed model based on an electronic circuit. The results will help to deepen the understanding of the NHSE and its manipulation.

DOI: [10.1103/PhysRevB.106.L161402](https://doi.org/10.1103/PhysRevB.106.L161402)

Introduction. Hermiticity of Hamiltonian has been regarded as a fundamental requirement in standard quantum mechanics, and it ensures the conservation of probability and limits energy values to be real in isolated systems. However, many systems, such as the nonequilibrium and open systems with gain and loss, can be effectively described by non-Hermitian Hamiltonians. Especially in recent years, non-Hermitian physics has attracted widespread attention in both theory [1–16] and experiment [17–24]. Various unique features of non-Hermitian systems without any Hermitian counterparts have been revealed, such as exceptional points and rings [25–34], enriched topological classifications [35–40], and the non-Hermitian skin effect (NHSE) [7,8,10,21,41–46]. NHSE, namely that a majority of eigenstates are localized near the boundary under open boundary conditions (OBC), is one of the most iconic properties of non-Hermitian systems. It drastically reshapes the bulk-boundary correspondence principle and motivates the establishment of a generalized Brillouin zone [7–9]. The interplay between the NHSE and other fundamental phenomena (e.g., localization induced by external magnetic fields, defects, disorder, and quasiperiodic potentials [12–15,46–50]) has also attracted widespread attention recently. On the other hand, electric field can induce the Stark localization or dynamical localization and is also a frequently used fundamental method to manipulate other physical effects, since it is easily realized and controlled. However, the effect of electric fields on NHSE was not considered before.

Now we focus on how to manipulate NHSE by using electric fields. If the NHSE can be fully suppressed in the modulation process, the non-Hermitian effect may be eliminated, and the system may have the conservation of probability and all the eigenvalues may become real, even though the non-Hermitian term remains. Thus manipulating NHSE is helpful for deepening our understanding of non-Hermitian quantum mechanics and the differences between Hermitian and non-Hermitian physics. Moreover, mastering how to control NHSE, we will be able to obtain or remove it on demand. Therefore, manipulating NHSE also has practical significance. In this work, we want to address whether electric fields can manipulate NHSE and, furthermore, if they can, whether richer and more interesting physics and applications will emerge in light of this.

Model and results. We consider a one dimensional non-Hermitian system with nonreciprocal hopping under the influence of electric fields, and the Hamiltonian is written as

$$\hat{H} = \sum_n (J_L |n\rangle \langle n+1| + J_R |n+1\rangle \langle n|) + E(t)a \sum_n n |n\rangle \langle n|, \quad (1)$$

where $|n\rangle$ is the Wannier state localized on the lattice site n , $J_L(J_R)$ represents the leftward (rightward) hopping amplitude, a is the lattice constant, being set as 1 throughout this work, and $E(t) = e\xi(t)$, with e and $\xi(t)$ being the particle's charge and external electric field, respectively.

We can analytically confirm the existence or disappearance of NHSE by investigating the motion of a particle; this is because the particle initially localized in the bulk should move toward the boundary if the NHSE exists. We first substitute an arbitrary time-dependent quantum state $|\psi(t)\rangle = \sum_m C_m(t)|m\rangle$ into the Schrödinger equation $i\partial_t |\psi(t)\rangle =$

^{*}These authors contributed equally to this work.

[†]Corresponding author: wangyc3@sustech.edu.cn

$\hat{H}(t)|\psi(t)\rangle$ and obtain the equation of motion for the time-dependent amplitudes $C_m(t)$:

$$i\partial_t C_m(t) = J_L C_{m+1}(t) + J_R C_{m-1}(t) + mE(t)C_m(t). \quad (2)$$

Here we set $\hbar = 1$. By solving Eq. (2), for arbitrary $E(t)$, we can obtain the exact solutions:

$$C_m(t) = \sum_n (-1)^{m-n} C_n(0) e^{-i\eta(t)n} \mathcal{J}_{m-n} \\ \times (2\sqrt{J_L J_R [U^2(t) + V^2(t)]}) \left[\frac{J_R iV(t) - U(t)}{J_L iV(t) + U(t)} \right]^{\frac{m-n}{2}}. \quad (3)$$

Here $\mathcal{J}_{m-n}(x)$ is the $(m-n)$ th order Bessel function of the first kind, $U(t) = \int_0^t \cos[\eta(t) - \eta(t')] dt'$ and $V(t) = \int_0^t \sin[\eta(t) - \eta(t')] dt'$ with

$$\eta(t) = \int_0^t E(t') dt'. \quad (4)$$

This solution is valid for arbitrary initial bulk state $|\psi(0)\rangle$ and arbitrary $E(t)$, and the calculation details are in the Supplemental Material [51]. To simplify the expression, without loss of generality, we consider a specific initial state that only occupies a single Wannier lattice site n_0 , namely $|\psi(0)\rangle = |n_0\rangle$, and then the probability at any site m after evolution time t , $\rho_m(t) = |C_m(t)|^2$, takes [51]

$$\rho_m(t) = \mathcal{J}_{m-n_0}^2 (2\sqrt{J_L J_R [u^2(t) + v^2(t)]}) \left(\frac{J_R}{J_L} \right)^{m-n_0}, \quad (5)$$

with

$$u(t) = \int_0^t dt' \cos \eta(t'), \quad v(t) = \int_0^t dt' \sin \eta(t'). \quad (6)$$

In the absence of electric fields, i.e., $E(t) = 0$, from Eq. (4) and Eq. (6), we have $u(t) = t$ and $v(t) = 0$, yielding $\rho_m(t) = \mathcal{J}_{m-n_0}^2 (2t\sqrt{J_L J_R}) (J_R/J_L)^{m-n_0}$, where $2t\sqrt{J_L J_R}$ linearly increases to infinity and thus $\mathcal{J}_{m-n_0}(2t\sqrt{J_L J_R})$ tends to 0 [52] [see Fig. 1(a)], such that $\rho_m/\rho_{m-1} \approx J_R/J_L$ when $t \rightarrow \infty$ [51]. Therefore, the system has right (left) boundary skin mode when $J_R/J_L > 1$ ($J_R/J_L < 1$), which is consistent with previous results [7,8,10]. The following sections will discuss three cases: (i) the pure dc field case, (ii) the pure ac field case, and (iii) the dc-ac mixed field case.

Pure dc electric field case. We first discuss the fate of NHSE in the presence of a pure dc electric field, i.e., $E(t) = E_0$. From Eq. (4) and Eq. (6), we have $u(t) = \sin(E_0 t)/E_0$ and $v(t) = (1 - \cos E_0 t)/E_0$, and then Eq. (5) gives the probability

$$\rho_m(t) = \mathcal{J}_{m-n_0}^2 \left(\frac{4\sqrt{J_L J_R}}{E_0} \sin \frac{E_0 t}{2} \right) \left(\frac{J_R}{J_L} \right)^{m-n_0}. \quad (7)$$

Note that $\sin(E_0 t^*/2) = 0$ at the time points $t^* = 2\pi N/E_0$ with $N = 0, 1, 2, \dots$. By using the properties of the Bessel function [52] $\mathcal{J}_{m-n_0}(0) = \delta_{m-n_0,0}$ [see Fig. 1(a)] and $(J_R/J_L)^{m-n_0} = 1$ when $m = n_0$, we have that $\rho_{m=n_0}(t^*)$ will oscillate back to 1 whatever the initial site n_0 is and this phenomenon is called Stark localization [53], which induces that the particle initially localized at the bulk does not move toward the boundary. Therefore, the effect of the interplay

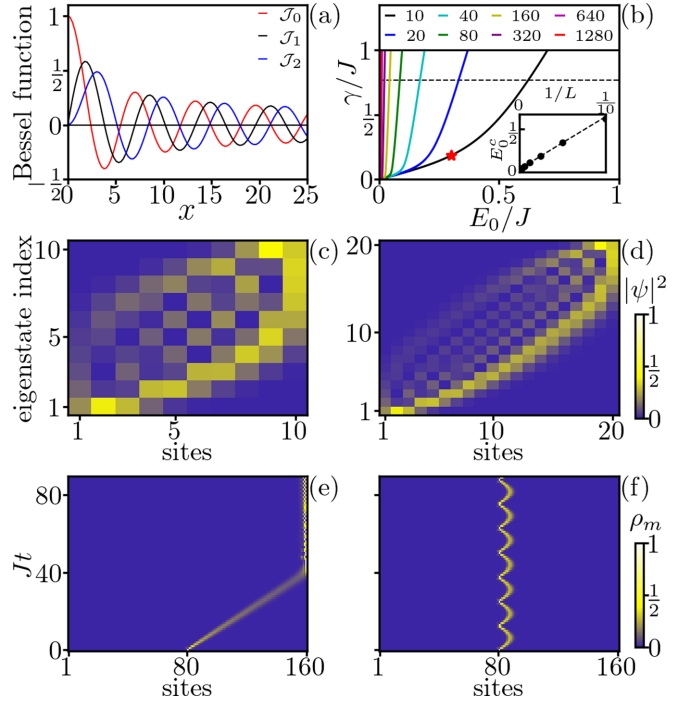


FIG. 1. (a) Distributions of the zeroth, first, and second order Bessel function. We can see two characteristics used in the text: the amplitudes of oscillation decrease with increasing x and when $x \rightarrow \infty$, $\mathcal{J}_m(x) \rightarrow 0$ for any m ; $\mathcal{J}_0(0) = 1$ and $\mathcal{J}_m(0) = 0$ when $m \neq 0$, so we have $\mathcal{J}_m(0) = \delta_{m,0}$. (b) Localization-delocalization transition characterized by winding number for finite lattices. The inset shows transition dc field strength E_0^c versus $1/L$, given $\gamma = 0.77$ marked as dashed line in its parent figure. The distributions of eigenstates with (c) $L = 10$ and (d) $L = 20$, and other parameters are $\gamma = 0.185$ and $E_0 = 0.3$ as marked by red star in (b). Dynamical evolution of a electron started from the lattice center under (e) the weak dc field with $E_0 = 0.005$ and (f) the strong dc field with $E_0 = 0.5$, and other parameters are $L = 160$ and $\gamma = 0.769$.

between the Stark localization and NHSE is that even a small dc field is sufficient to suppress the NHSE.

The analytical results can be further confirmed by numerically calculating the winding number (WN). To define the WN, we need to introduce the twist boundary condition here, i.e., $\hat{H}(\Phi) = \hat{H} + J_L e^{i\Phi} |L\rangle\langle 1| + J_R e^{-i\Phi} |1\rangle\langle L|$, where L is the system size and Φ is the introduced phase factor, and then the WN reads

$$w = \frac{1}{2\pi i} \int_0^{2\pi} \partial_\Phi \ln \det[\hat{H}(\Phi) - \mathcal{E}_c] d\Phi. \quad (8)$$

$w = 1$ ($w = 0$) corresponds to the existence (nonexistence) of NHSE under OBC with eigenvalue around \mathcal{E}_c [6,42,43,45], which is set to the algebra average of the spectrum in the following calculation. For convenience, we set $J_L = J - \gamma/2$ and $J_R = J + \gamma/2$ with $\gamma > 0$ and $J = 1$ as the unit of energy. Figure 1(b) shows the transition of the existence-nonexistence of NHSE, obtained by calculating the WN, which changes from 1 to 0 when the strength of dc field E_0 increases cross the transition line with fixed L from left to right. It can be seen that the transition lines tend to $E_0 = 0$ with increasing L , which is consistent with the analytical result.

The analytical expression of $\rho_m(t)$ can also tell us the finite size effect, where interesting physics will emerge. Here, we consider $J_R > J_L$, which makes the oscillation of the particle favor the right-hand side of the initial position n_0 , and the oscillation range is approximate to $4J_R/|E_0|x_*$ [51], where x_* only depends on J_L and J_R . If the distance between the right-side boundary and n_0 is larger than $4J_R/|E_0|x_*$, the particle will return back to n_0 after a period of time, but if the distance is less than $4J_R/|E_0|x_*$, the particle will arrive at the boundary and then stay there ever since. Thus, for fixed size L , there exist a critical electric field strength E_0^c that describes the transition of the existence-nonexistence of NHSE and satisfies $4J_R/|E_0^c|x_* = L$, giving $E_0^c \propto 1/L$, as shown in Fig. 1(b). When the size exceeds a critical value, the number of skin modes is about $4J_R/|E_0|x_*$, which is independent of the size. It can be clearly seen by comparing Figs. 1(c) and 1(d), which show the distributions of eigenstates with different sizes and the same other parameters, and having the same number of skin modes. Thus, with fixing J_L , J_R , and E_0 , the number of skin modes can be of the same order of magnitude as the total eigenstate number for the system with small size and the NHSE exists. When the size is large enough, the ratio of the number of skin modes to the total eigenstate number will be insignificant and the NHSE will disappear, suggesting that the NHSE is size dependent, which is different from the general NHSE. Moreover, we can increase the number of skin modes by decreasing the electric field strength and, thus, we can control the appearance or disappearance of NHSE for a finite size system, as shown in Figs. 1(e) and 1(f), where the system shows NHSE when $E_0 = 0.005$, but when $E_0 = 0.5$, the NHSE disappear. The phenomenon of the size-dependent NHSE should widely exist in the non-Hermitian systems with defective, disordered, quasiperiodic, or Stark potentials, or two coupled chains with dissimilar nonreciprocal hoppings [46].

Pure ac electric field case. We then consider the monochromatic cosine shape ac electric field $E(t) = E_1 \cos(\omega t)$. It is a typical Floquet driving system, with period $T = 2\pi/\omega$. From Eq. (4) and Eq. (6), we have $u(t) = \int_0^t dt' \cos(\frac{E_1}{\omega} \sin \omega t')$ and $v(t) = \int_0^t dt' \sin(\frac{E_1}{\omega} \sin \omega t')$, and then Eq. (5) gives the probability in the limit $t \gg T$ [51]:

$$\rho_m(t \gg T) \approx \mathcal{J}_{m-n_0}^2 \left[2t \sqrt{J_L J_R} \mathcal{J}_0 \left(\frac{E_1}{\omega} \right) \right] \left(\frac{J_R}{J_L} \right)^{m-n_0}. \quad (9)$$

When $\mathcal{J}_0(E_1/\omega) \neq 0$, $2t \sqrt{J_L J_R} \mathcal{J}_0(E_1/\omega)$ increases linearly to infinity and thus $\mathcal{J}_{m-n_0}[2t \sqrt{J_L J_R} \mathcal{J}_0(E_1/\omega)]$ tends to zero, which is completely similar to the case without electric field, suggesting that the NHSE is not affected by the ac field. For the special ac field strength E_1 and frequency ω that satisfy $\mathcal{J}_0(E_1/\omega) = 0$, corresponding to the red round dots in Fig. 2(a), due to $\mathcal{J}_{m-n_0}(0) = \delta_{m-n_0,0}$, the particle initially localized in the bulk will move around the initial position and thus the NHSE will be suppressed, as shown in Fig. 2(b). This localization phenomenon is called dynamic localization [54–57], which is distinct from Anderson localization induced by random disorder potential. For most cases, $\mathcal{J}_0(E_1/\omega) \neq 0$, the particle will hop to the boundary eventually as demonstrated in Fig. 2(c). To sum up, when only applying the ac electric field to the system, the NHSE is not affected except for

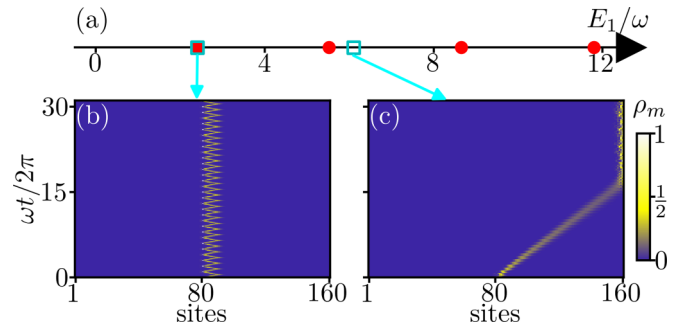


FIG. 2. (a) Red round dots are zeros of zeroth order of the Bessel function $\mathcal{J}_0(E_1/\omega)$, which correspond to the condition of the emergence of the dynamic localization under ac field driving. Dynamical evolution of a particle initially localized at the lattice center with (b) $E_1/\omega = 2.405$, which is the first zero point of $\mathcal{J}_0(E_1/\omega)$ and (c) $E_1/\omega = 6.1$. Here we set $J = 1$, $\gamma = 0.73$, and $\omega = 0.46$.

these special parameters of E_1 and ω that cause the dynamic localization, suppressing the NHSE.

dc+ac electric field case. We finally consider the effect of dc-ac mixed fields, i.e., $E(t) = E_0 + E_1 \cos(\omega t)$, in manipulating NHSE. By using Eq. (4) and Eq. (6), we can calculate functions $u(t)$ and $v(t)$, whose expressions look fairly complicated [51], and find that when E_0/ω is not an integer, all the terms in the expressions of $u(t)$ and $v(t)$ are bounded oscillatory functions of time, meaning that the particle will oscillate around the initial position. Therefore, the electric fields break NHSE for noninteger E_0/ω . When E_0/ω is an integer, the probability in the limit of long evolution time [51] can be simplified to

$$\rho_m(t \gg T) \approx \mathcal{J}_{m-n_0}^2 \left[2t \sqrt{J_L J_R} \mathcal{J}_{\frac{E_0}{\omega}} \left(\frac{E_1}{\omega} \right) \right] \left(\frac{J_R}{J_L} \right)^{m-n_0}. \quad (10)$$

Similar to the discussions for Eq. (9), the disappearance or existence of NHSE depends on whether E_1/ω is one of the zeros of the Bessel function $\mathcal{J}_{E_0/\omega}$. The pure dc field can cause the Stark localization, which suppresses NHSE. Then adding the ac field $E_1 \cos(\omega t)$ with E_0/ω being integers, the particle can break through the localization barrier and move through the chain accompanied by the photon absorption or emission. Thus NHSE can exist only for integer E_0/ω except for the situations in which E_1/ω are the zeros of $\mathcal{J}_{E_0/\omega}$, which will induce the dynamic localization, as discussed above. The effects of the dc-ac mixture fields on NHSE are summarized in Fig. 3(a). The light green region between the red lines and the dark green dots on the red lines respectively correspond to the noninteger E_0/ω and the zeros of $\mathcal{J}_{E_0/\omega}$ with E_0/ω being integers, which will induce the Stark localization and dynamic localization and lead to the disappearance of NHSE, as shown in Figs. 3(b) and 3(c). The red lines correspond to the integer E_0/ω , which can break the bulk localization by photon assisted hopping, and the particle initially localized in the bulk will move toward the boundary, as shown in Fig. 3(d).

Electronic circuit's realization. The non-Hermitian model (1) can be simulated by a classical electric circuit as depicted in Fig. 4, which consists of L LC circuit units. Based on the

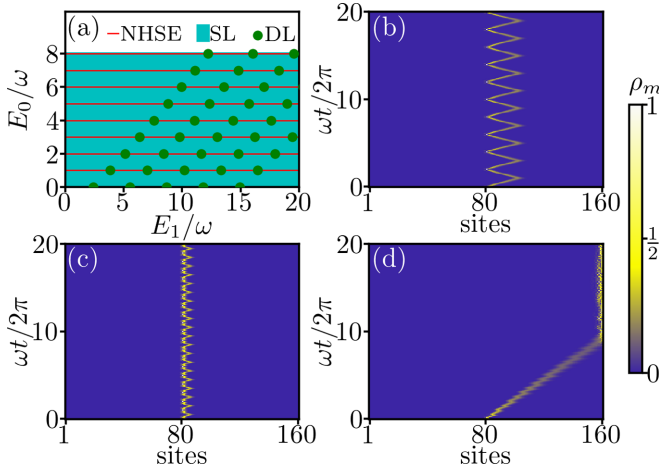


FIG. 3. (a) Schematic phase diagram about the existence or nonexistence of NHSE under the mixed electric field driving. Red lines represent the integer E_0/ω . Dark green dots on the red lines correspond to E_1/ω being the zeros of $\mathcal{J}_{E_0/\omega}$, where dynamic localization (DL) induced by the ac field occurs. The light green region corresponds to the Stark localization (SL). The dynamical evolutions of the electron initialized on the lattice center under simultaneous driving of dc and ac fields with (b) $E_0/\omega = 0.5$ and $E_1/\omega = 1.3$, (c) $E_0/\omega = 1$ and $E_1/\omega = 3.832$ corresponding to the first zero of \mathcal{J}_1 , and (d) $E_0/\omega = 1$ and $E_1/\omega = 5.7$. Here we fix $J = 1$, $\gamma = 0.73$, and $\omega = 0.46$.

Kirchhoff's current law, we have

$$I_n^R = I_n^L + I_n^B, \quad (11)$$

where I_n^B is the current flow through the n th unit and I_n^L (I_n^R) is the current from the $(n-1)$ th (n th) unit to the n th [$(n+1)$ th] unit, and they satisfy

$$L_n \frac{dI_n^L}{dt} = V_n - V_{n-1}, \quad L_{n+1} \frac{dI_n^R}{dt} = V_{n+1} - V_n, \quad (12)$$

$$l_n \frac{d}{dt} \left[I_n^B - C_n \frac{dV_n}{dt} \right] = V_n, \quad (13)$$

where V_n is the voltage on the node n . From Eqs. (11)–(13), one can obtain

$$\frac{d^2 V_n}{dt^2} = \frac{V_{n+1} - V_n}{C_n L_{n+1}} + \frac{V_{n-1} - V_n}{C_n L_n} - \frac{V_n}{C_n l_n}. \quad (14)$$

When choosing inductors with inductances $L_n = L_0 g^{-n}$, $l_n = L_n / (\Delta - a n E_0)$, and capacitors with capacitance

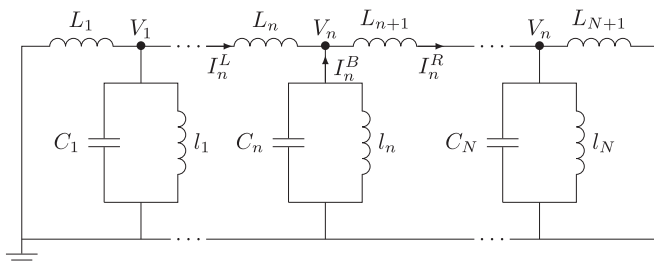


FIG. 4. Schematic of the LC electronic circuit.

$C_n = C_0 g^n$, Eq. (14) becomes

$$\left(1 + g + \Delta + \frac{1}{\omega_0^2} \frac{d^2}{dt^2} \right) V_n = V_{n-1} + g V_{n+1} + n a E_0 V_n, \quad (15)$$

where $\omega_0 = 1/\sqrt{C_0 L_0}$. We make a transformation: $V_n \rightarrow V_n e^{\pm i \omega t}$ with $n = 1, 2, \dots, L$ and $\omega = \omega_0 \sqrt{(1 + g + \Delta) - E_R}$; then Eq. (15) becomes $E_R V_n = V_{n-1} + g V_{n+1} + n a E_0 V_n$, which describes the dc case of the model (1) with $J_L = 1$ and $J_R = g$. By directly detecting the eigenvalues and eigenstates through an elementary voltage measurement [21], one can detect the manipulation effect of the dc field.

We note that our results can also apply to the manipulation of the NHSE induced by the on-site dissipations. Recent experiment [24] and theoretical proposals [58,59] suggest realizing and detecting the NHSE in the dissipative ultracold atom systems, where the gradient fields can be easily realized [60–62]. Therefore, the control effect of the electric fields on the NHSE can be detected in optical lattices. Furthermore, this control effect can also be detected based on the photonic quantum walk [19] and the sideband cooling setups in trapped ion systems [63,64].

Summary and discussion. We have investigated the control effect of electric fields on NHSE analytically and numerically. For the pure dc field case, in the thermodynamic limit, a weak Stark localization induced by the dc field is sufficient to win the competition with NHSE, so a nonzero dc field can suppress the NHSE. When the system size is finite, the new interesting phenomenon of the size-dependent NHSE will emerge, because the number of skin modes is size independent when the size exceeds a critical value. For the pure ac field case, only the special field strength E_1 and frequency ω that satisfy $\mathcal{J}_0(E_1/\omega) = 0$ can suppress the NHSE due to the dynamic localization. For the mixed field case, if E_0/ω is not an integer, the NHSE will be suppressed by the Stark localization induced by the dc field. For the integer E_0/ω , NHSE can exist, because the particle can move toward the boundary by the photon absorption or emission except for the special case with E_1/ω being one of the zeros of $\mathcal{J}_{E_0/\omega}$, which causes the dynamic localization.

The control effects of electric fields on the NHSE are abundant and, moreover, electric fields can be easily applied to a system. Thus the manipulation methods can be widely used in experiments and the fabrication of new devices. For instance, based on the phenomenon of the size-dependent NHSE and the sensitivity of the NHSE versus the field strength and frequency of ac fields near the special situations that satisfy $\mathcal{J}_0(E_1/\omega) = 0$, by detecting the signals on the boundary of a non-Hermitian system, one can carry out accurate measurements of electric fields, which are important for many critical applications in science and industry. As a second example, the NHSE can be used to design some devices, such as directional amplifiers [65–72] and light funnels [20]. The appearance or disappearance of the directional amplification and the funneling effect can be manipulated by using dc or ac fields, such as by changing the strength or frequency of an added ac field. Thus one can design the switch of these devices by using electric fields.

We thank L. Li and H. Jiang for valuable discussions. This work was supported by the National Natural Science Foundation of China (Grants No. U1801661, No.

12104205, and No. 12104210), the Key-Area Research and Development Program of Guangdong Province (Grant No. 2018B030326001), and Guangdong Provincial Key Laboratory (Grant No. 2019B121203002).

-
- [1] Y. Ashida, Z. Gong, and M. Ueda, Non-Hermitian physics, *Adv. Phys.* **69**, 249 (2020).
- [2] C. M. Bender and S. Boettcher, Real Spectra in Non-Hermitian Hamiltonians Having PT-symmetry, *Phys. Rev. Lett.* **80**, 5243 (1998); C. M. Bender, D. C. Brody, and H. F. Jones, Complex Extension of Quantum Mechanics, *ibid.* **89**, 270401 (2002).
- [3] N. Hatano and D. R. Nelson, Vortex pinning and non-Hermitian quantum mechanics, *Phys. Rev. B* **56**, 8651 (1997); Non-Hermitian delocalization and eigenfunctions, **58**, 8384 (1998).
- [4] T. E. Lee, Anomalous Edge State in a Non-Hermitian Lattice, *Phys. Rev. Lett.* **116**, 133903 (2016).
- [5] H. Shen, B. Zhen, and L. Fu, Topological Band Theory for Non-Hermitian Hamiltonians, *Phys. Rev. Lett.* **120**, 146402 (2018).
- [6] Z. Gong, Y. Ashida, K. Kawabata, K. Takasan, S. Higashikawa, and M. Ueda, Topological Phases of Non-Hermitian Systems, *Phys. Rev. X* **8**, 031079 (2018).
- [7] S. Yao and Z. Wang, Edge States and Topological Invariants of Non-Hermitian Systems, *Phys. Rev. Lett.* **121**, 086803 (2018); S. Yao, F. Song, and Z. Wang, Non-Hermitian Chern Bands, *ibid.* **121**, 136802 (2018).
- [8] F. K. Kunst, E. Edvardsson, J. C. Budich, and E. J. Bergholtz, Biorthogonal Bulk-Boundary Correspondence in Non-Hermitian Systems, *Phys. Rev. Lett.* **121**, 026808 (2018).
- [9] Z. Yang, K. Zhang, C. Fang, and J. Hu, Non-Hermitian Bulk-Boundary Correspondence and Auxiliary Generalized Brillouin Zone Theory, *Phys. Rev. Lett.* **125**, 226402 (2020).
- [10] C. H. Lee and R. Thomale, Anatomy of skin modes and topology in non-Hermitian systems, *Phys. Rev. B* **99**, 201103(R) (2019).
- [11] K. Kawabata, K. Shiozaki, M. Ueda, and M. Sato, Symmetry and Topology in Non-Hermitian Physics, *Phys. Rev. X* **9**, 041015 (2019).
- [12] S. Longhi, Topological Phase Transition in Non-Hermitian Quasicrystals, *Phys. Rev. Lett.* **122**, 237601 (2019); Phase transitions in a non-Hermitian Aubry-Andre-Harper model, *Phys. Rev. B* **103**, 054203 (2021).
- [13] H. Jiang, L.-J. Lang, C. Yang, S.-L. Zhu, and S. Chen, Interplay of non-Hermitian skin effects and Anderson localization in non-reciprocal quasiperiodic lattices, *Phys. Rev. B* **100**, 054301 (2019).
- [14] Y. Liu, X. Jiang, J. Cao, and S. Chen, Non-Hermitian mobility edges in one-dimensional quasicrystals with parity-time symmetry, *Phys. Rev. B* **101**, 174205 (2020); Y. Liu, Y. Wang, Z. Zheng, and S. Chen, Exact non-Hermitian mobility edges in one-dimensional quasicrystal lattice with exponentially decaying hopping and its dual lattice, *ibid.* **103**, 134208 (2021).
- [15] L. Zhou, Floquet engineering of topological localization transitions and mobility edges in one-dimensional non-Hermitian quasicrystals, *Phys. Rev. Res.* **3**, 033184 (2021).
- [16] E. J. Bergholtz, J. C. Budich, and F. K. Kunst, Exceptional topology of non-Hermitian systems, *Rev. Mod. Phys.* **93**, 015005 (2021).
- [17] H. Schomerus, Topologically protected midgap states in complex photonic lattices, *Opt. Lett.* **38**, 1912 (2013).
- [18] J. Li, A. K. Harter, J. Liu, L. de Melo, Y. N. Joglekar, and L. Luo, Observation of parity-time symmetry breaking transitions in a dissipative Floquet system of ultracold atoms, *Nat. Commun.* **10**, 855 (2019).
- [19] L. Xiao, T. Deng, K. Wang, G. Zhu, Z. Wang, W. Yi, and P. Xue, Non-Hermitian bulk-boundary correspondence in quantum dynamics, *Nat. Phys.* **16**, 761 (2020).
- [20] S. Weidemann, M. Kremer, T. Helbig, T. Hofmann, A. Stegmaier, M. Greiter, R. Thomale, and A. Szameit, Topological funneling of light, *Science* **368**, 311 (2020).
- [21] T. Helbig, T. Hofmann, S. Imhof, M. Abdelghany, T. Kiessling, L. Molenkamp, C. Lee, A. Szameit, M. Greiter, and R. Thomale, Generalized bulk-boundary correspondence in non-Hermitian topoelectrical circuits, *Nat. Phys.* **16**, 747 (2020).
- [22] X.-X. Zhang and M. Franz, Non-Hermitian Exceptional Landau Quantization in Electric Circuits, *Phys. Rev. Lett.* **124**, 046401 (2020).
- [23] W. Zhang, X. Ouyang, X. Huang, X. Wang, H. Zhang, Y. Yu, X. Chang, Y. Liu, D.-L. Deng, and L.-M. Duan, Observation of Non-Hermitian Topology with Nonunitary Dynamics of Solid-State Spins, *Phys. Rev. Lett.* **127**, 090501 (2021).
- [24] Q. Liang, D. Xie, Z. Dong, H. Li, H. Li, B. Gadway, W. Yi, and B. Yan, Dynamic Signatures of Non-Hermitian Skin Effect and Topology in Ultracold Atoms, *Phys. Rev. Lett.* **129**, 070401 (2022).
- [25] C. Dembowski, H.-D. Gräf, H. L. Harney, A. Heine, W. D. Heiss, H. Rehfeld, and A. Richter, Experimental Observation of the Topological Structure of Exceptional Points, *Phys. Rev. Lett.* **86**, 787 (2001); C. Dembowski, B. Dietz, H.-D. Gräf, H. L. Harney, A. Heine, W. D. Heiss, and A. Richter, Encircling an exceptional point, *Phys. Rev. E* **69**, 056216 (2004).
- [26] J. Wiersig, Enhancing the Sensitivity of Frequency and Energy Splitting Detection by Using Exceptional Points: Application to Microcavity Sensors for Single-Particle Detection, *Phys. Rev. Lett.* **112**, 203901 (2014).
- [27] W. Hu, H. Wang, P. P. Shum, and Y. D. Chong, Exceptional points in a non-Hermitian topological pump, *Phys. Rev. B* **95**, 184306 (2017).
- [28] W. Chen, Ş. K. Özdemir, G. Zhao, J. Wiersig, and L. Yang, Exceptional points enhance sensing in an optical microcavity, *Nature (London)* **548**, 192 (2017).
- [29] H. Hodaie, A. U. Hassan, S. Wittek, H. Garcia-Gracia, R. El-Ganainy, D. N. Christodoulides, and M. Khajavikhan, Enhanced sensitivity at higher-order exceptional points, *Nature (London)* **548**, 187 (2017).

- [30] M. Zhang, W. Sweeney, C. W. Hsu, L. Yang, A. D. Stone, and L. Jiang, Quantum Noise Theory of Exceptional Point Amplifying Sensors, *Phys. Rev. Lett.* **123**, 180501 (2019).
- [31] M.-A. Miri and A. Alù, Exceptional points in optics and photonics, *Science* **363**, eaar7709 (2019).
- [32] Y. Xu, S.-T. Wang, and L.-M. Duan, Weyl Exceptional Rings in a Three-Dimensional Dissipative Cold Atomic Gas, *Phys. Rev. Lett.* **118**, 045701 (2017).
- [33] A. Cerjan, S. Huang, M. Wang, K. P. Chen, Y. Chong, and M. C. Rechtsman, Experimental realization of a Weyl exceptional ring, *Nat. Photon.* **13**, 623 (2019).
- [34] C. H. Lee, L. Li, and J. Gong, Hybrid Higher-Order Skin-Topological Modes in Nonreciprocal Systems, *Phys. Rev. Lett.* **123**, 016805 (2019).
- [35] K. Kawabata, S. Higashikawa, Z. Gong, Y. Ashida, and M. Ueda, Topological unification of time-reversal and particle-hole symmetries in non-Hermitian physics, *Nat. Commun.* **10**, 297 (2019).
- [36] U. Magnea, Random matrices beyond the Cartan classification, *J. Phys. A: Math. Theor.* **41**, 045203 (2008).
- [37] C. C. Wojcik, X.-Q. Sun, T. Bzdušek, and S. Fan, Homotopy characterization of non-Hermitian Hamiltonians, *Phys. Rev. B* **101**, 205417 (2020).
- [38] Z. Li and R. S. K. Mong, Homotopical classification of non-Hermitian band structures, *Phys. Rev. B* **103**, 155129 (2021).
- [39] H. Hu and E. Zhao, Knots and Non-Hermitian Bloch Bands, *Phys. Rev. Lett.* **126**, 010401 (2021).
- [40] C.-H. Liu and S. Chen, Topological classification of defects in non-Hermitian systems, *Phys. Rev. B* **100**, 144106 (2019); C.-H. Liu, H. Jiang, and S. Chen, Topological classification of non-Hermitian systems with reflection symmetry, *ibid.* **99**, 125103 (2019).
- [41] V. M. Martínez Alvarez, J. E. Barrios Vargas, and L. E. F. Foa Torres, Non-Hermitian robust edge states in one dimension: Anomalous localization and eigenspace condensation at exceptional points, *Phys. Rev. B* **97**, 121401(R) (2018).
- [42] D. S. Borgnia, A. J. Kruchkov, and R.-J. Slager, Non-Hermitian Boundary Modes and Topology, *Phys. Rev. Lett.* **124**, 056802 (2020).
- [43] K. Zhang, Z. Yang, and C. Fang, Correspondence between Winding Numbers and Skin Modes in Non-Hermitian Systems, *Phys. Rev. Lett.* **125**, 126402 (2020); Universal non-Hermitian skin effect in two and higher dimensions, *Nat. Commun.* **13**, 2496 (2022).
- [44] Y. Yi and Z. Yang, Non-Hermitian Skin Modes Induced by On-Site Dissipations and Chiral Tunneling Effect, *Phys. Rev. Lett.* **125**, 186802 (2020).
- [45] N. Okuma, K. Kawabata, K. Shiozaki, and M. Sato, Topological Origin of non-Hermitian Skin Effects, *Phys. Rev. Lett.* **124**, 086801 (2020).
- [46] L. Li, C. H. Lee, S. Mu, and J. Gong, Critical non-Hermitian skin effect, *Nat. Commun.* **11**, 5491 (2020); L. Li, C. H. Lee, and J. Gong, Impurity induced scale-free localization, *Commun. Phys.* **4**, 42 (2021).
- [47] M. Lu, X.-X. Zhang, and M. Franz, Magnetic Suppression of Non-Hermitian Skin Effects, *Phys. Rev. Lett.* **127**, 256402 (2021).
- [48] K. Shao, H. Geng, W. Chen, and D. Y. Xing, Interplay between non-Hermitian skin effect and magnetic field: skin modes suppression, Onsager quantization and MT phase transition, *Phys. Rev. B* **106**, L081402 (2022).
- [49] X.-Q. Sun, P. Zhu, and T. L. Hughes, Geometric Response and Disclination-Induced Skin Effects in Non-Hermitian Systems, *Phys. Rev. Lett.* **127**, 066401 (2021).
- [50] R. Hamazaki, K. Kawabata, and M. Ueda, Non-Hermitian Many-Body Localization, *Phys. Rev. Lett.* **123**, 090603 (2019).
- [51] See Supplemental Material at <http://link.aps.org/supplemental/10.1103/PhysRevB.106.L161402> for details on (I) deriving the analytical solutions of quantum dynamics, (II) discussing the analytical results, (III) the finite size effect in the pure dc field case, and (IV) dynamical behavior in the absence of external fields. The Supplemental Material includes Refs. [52,73,74].
- [52] G. N. Watson, *A Treatise on the Theory of Bessel Functions*, Cambridge Mathematical Library (Cambridge University Press, Cambridge, UK, 1995).
- [53] G. H. Wannier, Dynamics of band electrons in electric and magnetic fields, *Rev. Mod. Phys.* **34**, 645 (1962).
- [54] D. H. Dunlap and V. M. Kenkre, Dynamic localization of a charged particle moving under the influence of an electric field, *Phys. Rev. B* **34**, 3625 (1986); Dynamic localization of a particle in an electric field viewed in momentum space: Connection with Bloch oscillations, *Phys. Lett. A* **127**, 438 (1988).
- [55] X.-G. Zhao, R. Jahnke, and Q. Niu, Dynamic fractional stark ladders in dc-ac fields, *Phys. Lett. A* **202**, 297 (1995); X.-G. Zhao, G. A. Georgakis, and Q. Niu, Rabi oscillations between Bloch bands, *Phys. Rev. B* **54**, R5235 (1996).
- [56] S. Longhi, M. Marangoni, M. Lobino, R. Ramponi, P. Laporta, E. Cianci, and V. Foglietti, Observation of Dynamic Localization in Periodically Curved Waveguide Arrays, *Phys. Rev. Lett.* **96**, 243901 (2006).
- [57] A. Eckardt, M. Holthaus, H. Lignier, A. Zenesini, D. Ciampini, O. Morsch, and E. Arimondo, Exploring dynamic localization with a Bose-Einstein condensate, *Phys. Rev. A* **79**, 013611 (2009).
- [58] S. Guo, C. Dong, F. Zhang, J. Hu, and Z. Yang, Theoretical prediction of non-Hermitian skin effect in ultracold atom systems, [arXiv:2111.04220](https://arxiv.org/abs/2111.04220).
- [59] L. Zhou, H. Li, W. Yi, and X. Cui, Engineering non-Hermitian skin effect with band topology in ultracold gases, [arXiv:2111.04196](https://arxiv.org/abs/2111.04196).
- [60] C. Sias, H. Lignier, Y. P. Singh, A. Zenesini, D. Ciampini, O. Morsch, and E. Arimondo, Observation of Photon-Assisted Tunneling in Optical Lattices, *Phys. Rev. Lett.* **100**, 040404 (2008).
- [61] H. Miyake, G. A. Siviloglou, C. J. Kennedy, W. C. Burton, and W. Ketterle, Realizing the Harper Hamiltonian with Laser-Assisted Tunneling in Optical Lattices, *Phys. Rev. Lett.* **111**, 185302 (2013).
- [62] M. Aidelsburger, M. Atala, M. Lohse, J. T. Barreiro, B. Paredes, and I. Bloch, Realization of the Hofstadter Hamiltonian with Ultracold Atoms in Optical Lattices, *Phys. Rev. Lett.* **111**, 185301 (2013).
- [63] D. Leibfried, R. Blatt, C. Monroe, and D. Wineland, Quantum dynamics of single trapped ions, *Rev. Mod. Phys.* **75**, 281 (2003).
- [64] Z. Wang, Y. Peng, Y. Lu, Y. Wang, and J. Jie (unpublished).
- [65] A. Metelmann and A. A. Clerk, Nonreciprocal Photon Transmission and Amplification Via Reservoir Engineering, *Phys. Rev. X* **5**, 021025 (2015).

- [66] K. Fang, J. Luo, A. Metelmann, M. H. Matheny, F. Marquardt, A. A. Clerk, and O. Painter, Generalized non-reciprocity in an optomechanical circuit via synthetic magnetism and reservoir engineering, *Nat. Phys.* **13**, 465 (2017).
- [67] G. A. Peterson, F. Lecocq, K. Cicak, R. W. Simmonds, J. Aumentado, and J. D. Teufel, Demonstration of Efficient Non-reciprocity in a Microwave Optomechanical Circuit, *Phys. Rev. X* **7**, 031001 (2017).
- [68] S. Barzanjeh, M. Aquilina, and A. Xuereb, Manipulating the Flow of Thermal Noise in Quantum Devices, *Phys. Rev. Lett.* **120**, 060601 (2018).
- [69] A. McDonald, T. Pereg-Barnea, and A. A. Clerk, Phase-Dependent Chiral Transport and Effective Non-Hermitian Dynamics in a Bosonic Kitaev-Majorana Chain, *Phys. Rev. X* **8**, 041031 (2018).
- [70] D. Malz, L. D. Tóth, N. R. Bernier, A. K. Feofanov, T. J. Kippenberg, and A. Nunnenkamp, Quantum-Limited Directional Amplifiers with Optomechanics, *Phys. Rev. Lett.* **120**, 023601 (2018).
- [71] H. Xu, L. Jiang, A. A. Clerk, and J. G. E. Harris, Nonreciprocal control and cooling of phonon modes in an optomechanical system, *Nature (London)* **568**, 65 (2019).
- [72] W.-T. Xue, M.-R. Li, Y.-M. Hu, F. Song, and Z. Wang, Simple formulas of directional amplification from non-Bloch band theory, *Phys. Rev. B* **103**, L241408 (2021).
- [73] R. B. Paris, An inequality for the Bessel function $J_\nu(\nu x)$, *SIAM J. Math. Anal.* **15**, 203 (1984).
- [74] F. W. J. Olver, D. W. Lozier, and R. F. Boisvert, *NIST Handbook of Mathematical Functions* (Cambridge University Press, Cambridge, UK, 2010).